IJISET - International Journal of Innovative Science, Engineering & Technology, Vol. 2 Issue 11, November 2015.
www.ijiset.com
ISSN 2348 – 7968

Computational modeling and experimental analysis of counter electrode at its optimal temperature for quantum dot sensitized solar cells

Dinah Punnoose[1], Hee-Je Kim[2] and Sang-Hwa Chung[3*]

[1] Department of electrical and computer engineering, Pusan national university,2,Busandaehak-ro,63 beon-gil,Geumjeong-gu,Busan,46241,Rep.of KOREA,

[2]Department of electrical and computer engineering, Pusan national university,2,Busandaehak-ro,63 beon-gil,Geumjeong-gu,Busan,46241,Rep.of KOREA,

[3]Department of computer engineering, Pusan national university,2,Busandaehak-ro,63 beon-gil,Geumjeong-gu,Busan,46241,Rep.of KOREA,

Abstract

In this study, nickel sulfide (NiS) counter electrode (CE) was employed in quantum dot-sensitized solar cells (QDSSCs) in order to enhance the short circuit current, fill factor (FF) and power conversion efficiency (PCE). The NiS electrodes were prepared using chemical bath deposition method at varying temperatures before they were exploited. We computationally modeled the deposition temperature of the CE and simulation analysis of the same was examined. A circuit based simulation model for a solar cell in order to estimate the electrical behavior with respect to temperature and irradiance. This model was implemented on matlab simulink script file on the basis of parameter extraction from experimental data which accepts irradiance and temperature as variable parameters and outputs the I-V characteristics. The optimized CE exhibited an appreciated PCE of 3.30% under 1 sun illumination (AM 1.5G, 100 mW cm−2) and is superior to the cell employing platinized CE (1.89%).

.

Keywords: *Nickel sulfide; Counter electrode; Modeling; Quantum dot-sensitized solar cells; Matlab Simulink*

1. Introduction

Quantum dot sensitized solar cells (QDSSCs), in which semiconductor quantum dots (QDs) of narrow band gap function as photosensitizer, have of late attracted mounting interests as an alternative to the conventional dye-sensitized solar cell (DSSC), owing to their tunable band gap, large light absorption coefficient and high stability [1-7]. Successive ionic layer adsorption and reaction (SILAR) [8] and chemical bath deposition (CBD) [9] are frequently used methods for growing semiconductor QDs directly onto a mesoscopic oxide films. The most prominent QDs are metal sulfides and selenid es. Preceding research reports show that combination of QDs lead to higher efficiencies than pure materials [10, 11-14]. CdS, CdSe, PbS, PbSe and Sb2S3 are recurrently used as sensitizers in QDSSC's .Nevertheless, in-organic semi-conductor sensitizers, typically referred to as quantum dot (QD) sensitizers, are lately studied with great interest and surpass their dye homologues.

Many novel CEs have been reported to enhance the efficiency and fill factor (FF) of solar cells, such as Au, Cu2S, NiS, FeS, and CoS [12, 15-19]. Yang et al. reported the photovoltaic properties of CoS, CuS, and NiS CEs, and established that CoS is superior to the other two, in the order of CoS>CuS>NiS [20]. Among these, Ni is an abundant material in earth than Cu, Co and Pb.Batabyal et al. have reported that the nickel chalcogenides based nano-material's shows superior electro catalytic activity and good electrical properties for the iodine/iodide redox reactions than that of cobalt and copper chalcogenides in DSSC system [17]. In the present work, we investigated NiS CEs owing to their low cost, high electro-catalytic effect towards polysulfide reaction, and superior chemical activity [21]. We deposited NiS thin film by CBD because this process is low-cost, simple and low-temperature and has potential for large-scale production. Platinum (Pt) is the most precious of all electro-catalysts but however is not a good choice in QDSSCs employing polysulfide electrolytes. The construction of an efficient cathode is essential not only for QDSSCs but for all types of electrochemical cells. The present work, opts for the employment of NiS as efficient CE based on the deposition temperature . The deposition temperature of the NiS CE during chemical bath deposition (CBD) was varied in order to improve the efficiency and to replace the Pt CE.In addition, the performance of a solar cell is analyzed

ISSN 2348 – 7968

as a function of the CE deposition temperature. Various experiments are carried out to study the effects of the solar cell performance. Therefore a solar cell modeling needs to be developed to facilitate such experiments. A simulation model for the solar cell was implemented using the matlab software on the basis of this experimental data. A matlab simulink solar cell model that behaves accurately under variety of situations is developed and discussed in this paper. Consequently, our researchers testified that it is possible to hike the efficiency of a QDSSC by tuning the CE deposition temperature experimentally [21]. Present work takes into account both the temperature and irradiance into account. These effects are investigated and a new solar cell model is proposed. Equivalent circuit of a solar cell has been used for analytical and statistical analysis of the experimental data. This model was implemented on matlab simulink script file on the basis of parameter extraction from experimental data which accepts irradiance and temperature as variable parameters and outputs the I-V characteristics.

2. Simulation and experiment

2.1 Solar cell simulation

The equivalent circuit of the solar cell is shown below in Fig. 1, consisting of one current source, one diode element, resistances and capacitors [22–24]. The current source describes the photo-generated current (I_{PH}) by light irradiation. The resistances include a shunt resistance (R_{SH}) and a series resistance (R_S).

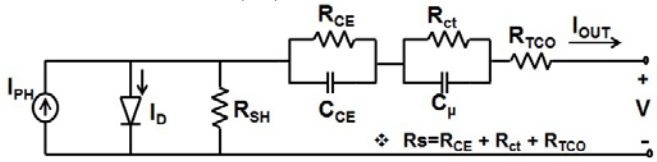

Fig. 1 Conventional equivalent circuit of a QDSSC

R_{SH} is related to the electron recombination across the TiO_2/dye/electrolyte interface. R_S includes three resistances, the resistances related to charge transport at the counter electrode (R_{CE}), resistance related to carrier transport by ions within the electrolyte (Rct) and the sheet resistance of the transparent conductive oxide (R_{TCO}).Capacitances are generally ignored in the DC analysis because they are very large [25]. Therefore, the diode current I_D is expressed as

$$I_D = I_0 \left\{ \exp\left(q \frac{V + I_{OUT} R_s}{nkT} \right) - 1 \right\} \quad (1)$$

where I_0 is the diode saturation current, q is the elementary charge, n is the ideality factor, k is the Boltzmann constant, and T is the temperature. Consequently, the output current (I_{OUT}) is described by

$$I_{OUT} = I_{PH} - I_0 \left\{ exp\left(q \frac{V + I_{OUT} R_s}{nkT} \right) - 1 \right\} - \frac{V + I_{OUT} R_s}{R_{CE}} \quad (2)$$

In an ideal cell Rs = Rsh = 0, which is a relatively common assumption [26]. For this paper, a model of moderate complexity was used. The net current of the cell is the difference of the photocurrent, IPH and the normal diode current I_D. The I–V characteristics of a QDSSC is nonlinear due to the term ID in the output current equation described in (2). This is difficult to simulate as the simulation process involving nonlinear equations is complicated and time consuming. In our study, the QDSSC simulation was carried out using matlab software. The model included temperature dependence of the photocurrent I_{PH} and the saturation current of the diode I_D for a certain ambient irradiation G, G_{nom} for the nominal value and Jsc as the current density.

$$I_{PH} = I_{PH}(T_1) + K_0(T - T_1) \quad (3)$$

$$I_{PH}(T_1) = J_{SC}(T_{1,nom}) \frac{G}{G_{nom}} \quad (4)$$

$$K_0 = \frac{J_{SC}(T_2) - J_{SC}(T_1)}{(T_2 - T_1)} \quad (5)$$

$$I_D = I_D(T_1) * \left(\frac{T}{T_1} \right)^{3/n} e^{\frac{qV_q(T_1)}{nk\left(\frac{1}{T} - \frac{1}{T_1}\right)}} \quad (6)$$

$$I_D(T_1) = \frac{J_{SC}(T_1)}{e^{\frac{qV(T_1)}{nKT_1}} - 1} \quad (7)$$

The simulated performance of a QDSSC as a function of CE deposition temperature results from calculating the values .The simulation process was coded using matlab script. The net current of the cell is the difference of the photocurrent, I_{PH} and the normal diode current I_D. A

ISSN 2348 – 7968

typical I-V characteristic of the solar cell for a certain ambient irradiation G and a certain fixed cell temperature. It should be pointed out that the power delivered to the load depends on the value of the resistance only. The open circuit voltage increases logarithmically with the ambient irradiation, while the short circuit current is a linear function of the ambient irradiation. The dominant effect with increasing cell's temperature is the linear decrease of the open circuit voltage, the cell being thus less efficient. The short circuit current slightly increases with the temperature.

2.2 Solar cell model implementation

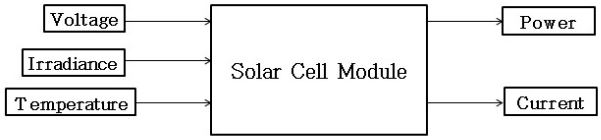

Fig. 2. Model of a solar cell using the matlab simulink tool

Fig. 2, shows the designed model of a solar cell using the matlab software. The investigated outputs of the solar cell module include the instantaneous power and current characteristics. These parameters vary according to the input parameters such as temperature, voltage and irradiance. Two scenarios were simulated. First the temperature was varied and in second instance the irradiation was varied to show the effect of solar radiation on the cells.

2.3 Experimental Section

Single cells with an active area of 0.27 cm2 were fabricated by depositing titanium dioxide (TiO_2) paste on a clean fluorine-doped tin oxide (FTO) by doctor blade method. Nano-porous TiO_2 structure was formed by sintering at 450 °C for 30 minutes and the final thickness was found to be ~7.5 µm after solvent evaporation. The TiO_2 electrodes were then sequentially sensitized with CdS and CdSe QDs using SILAR technique [8] and were carried out for 5 and 7 cycles respectively. Finally a passivating layer of ZnS was coated using the same technique. The resulting structure functions as a photo-anode. Separate NiS CEs were fabricated using chemical bath deposition (CBD) at deposition temperatures of 80, 90 and 100 °C for 90 minutes each. Finally, the NiS-coated films were washed several times with distilled water and were christened as NiS 80, NiS 90 and NiS 100 respectively and were used for further characterization.

3. Measurements

The TiO_2 thickness was measured using a surface profiler (ET4000, Dong-Il Techno Co. Ltd., Korea). The simulation results were displayed using the Simview program in the PSIM simulation tool. The absorbance of the CE with different temperatures was measured using a UV–vis spectrophotometer (Optizen 3220UV, Mecasys, Korea) at wavelengths ranging from 300 to 900 nm in order to analyze the performance of each sample. The photovoltaic performance of the fabricated cells and modules was measured under 1 sun illumination (air mass (AM) 1.5, 100 mW/cm^2) using a source meter (Model 2400, keithley Instrument Inc., USA .The I–V characteristics of each sample was represented as the open circuit voltage (V_{OC}), current density (J_{SC}), fill factor (FF) and conversion efficiency(η). Electrochemical impedance spectroscopy(EIS) was performed using a BioLogic potentiostat / EIS analyzer (SP-150, France).

4. Results and discussion

Scanning electron microscopy (SEM) was performed to study the formation of NiS on a fluorine-doped tin oxide (FTO) substrate. A top-view SEM image of the NiS CE is shown in Fig. 3, no thin film formation was observed on FTO substrate at 80 °C deposition temperature. However, at 90°C (NiS 90) NiS nanoparticles are formed on the FTO substrate and the size of the particles varied between 125-150 nm and is shown in Fig. 3b. But at the deposition temperature 90°C (NiS 90), the morphology of agglomerate nanoparticles was observed with the particle size of 263 nm. The NiS 90 CE shows the nano porous structure with a larger surface area, which renders high catalytic activity to the CE.

ISSN 2348 – 7968

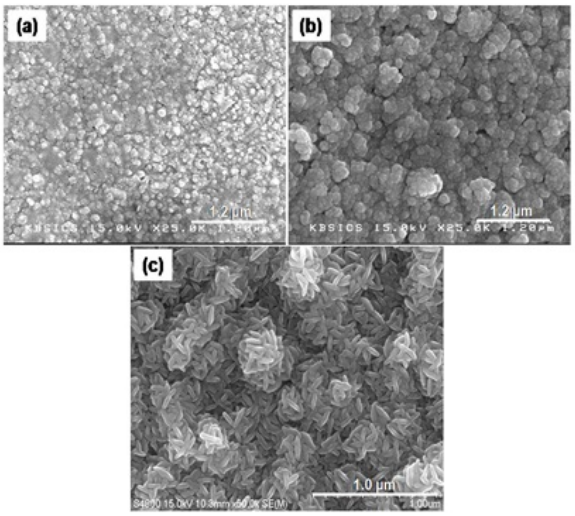

Fig. 3. The SEM images of the NiS thin film on FTO electrode: (a) NiS 80, (b) NiS 90, and (c) NiS 100.

When the deposition temperature at 100°C different type of morphology was observed on FTO and the SEM image is shown in Fig. 3c, the deposition temperature contributes to the surface change from nanoparticles to nano-flowers. When the deposition temperature was increased beyond 100 °C, the NiS started to peel off from the FTO substrate. We obtained good adhesion of the thin NiS layers deposited at 80 to 100 °C on the FTO substrate. When the deposition temperature increased more than 100°C, the NiS starts to peel off from FTO substrate. In the present work, we obtained good adhesion of NiS thin layer deposited at 80°C and 90°C on the FTO substrate. The degree of adhesion of the active materials (NiS) on FTO used as the CE is the crucial factor in determining the efficiency of the QDSSCs. If the materials do not stick to the FTO, they may be peeled off from the FTO substrate and released into the electrolyte, thereby decreasing the efficiency of the QDSSCs.

The current density –voltage characteristics of NiS CE is shown in Fig. 4.The efficiency (η), fill factor (FF), open circuit voltage (V_{oc}), and current density (J_{sc}) are summarized in Table 1. Higher performance with a conversion efficiency η of 3.30%, V_{oc} of 0.502 V, and J_{sc} of 13.70 mA cm^{-2} was obtained for the QDSSC fabricated using the NiS 90 CE. This is primarily because of the relatively low charge transfer resistance at the interface of the CE and electrolyte. Meanwhile, the NiS 80 and NiS 100 CEs exhibited η values of 2.47% and 2.67%, indicating moderate electro-catalytic activity for the redox polysulfide electrolyte.

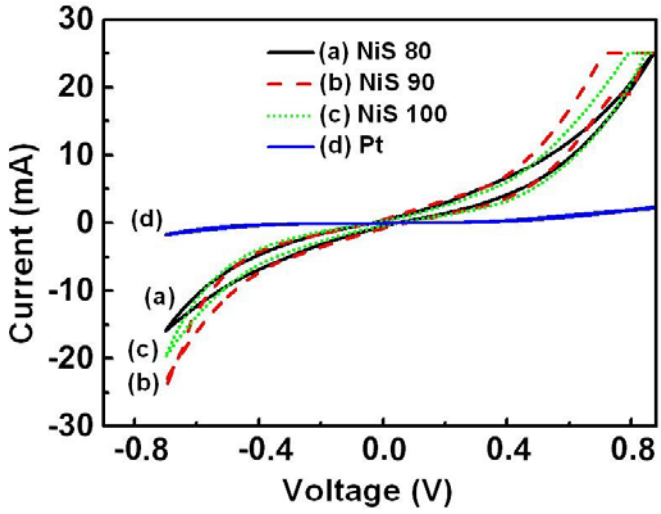

Fig. 4. The current density –voltage characteristics of NiS CE

The QDSSC, based on the Pt CE exhibited a higher V_{oc} of 0.624 V and moderate J_{sc} of 9.12 mA cm-2, but a very low FF of 0.330,which results in a low η of 1.89%. When NiS 90 and NiS 100 were used as CEs, the η of QDSSCs improved significantly compared to those of QDSSCs made using the NiS 80 and Pt CEs. The poorer performance of the Pt CE is due to the strong adsorption of sulfur compounds on the surface of the Pt, which reduces the surface activity and the conductivity of the Pt CE [16]. As a result, a low FF (0.33) is achieved by the Pt CE-based QDSSCs. The photovoltaic results indicate that the NiS 90 acts as an efficient CE for the QDSSC.

ISSN 2348 – 7968

TABLE 1

NiS and Pt CE based QDSSCs, their respective I-V characteristics and impedance data

Fig. 5, shows the simulated I-V, PV curves and performance of the QDSSC with different deposition temperatures 80, 90 and 100 °C. The simulated I–V characteristics coincided with the experimental tendency. The simulation method in this study is suitable for simulating the I–V characteristics of a QDSSC according to the deposition temperature. These extracted data from experiment were applied to the module in matlab in order to simulate the performance of the solar cell. From the comparison, it is seen that an increase in temperature leads to an increase in the open circuit voltage and a slight decrease in the short circuit current. Table 1 shows the I–V characteristics of quantum dot sensitized NiS CE from the experimental samples. The QDSSC was found to be more efficient when employing NiS CE fabricated at deposition temperature of 90 °C. It showed high η (%) when compared to that of Pt CE. As the J_{SC} value increases there is also an increase in the efficiency

.

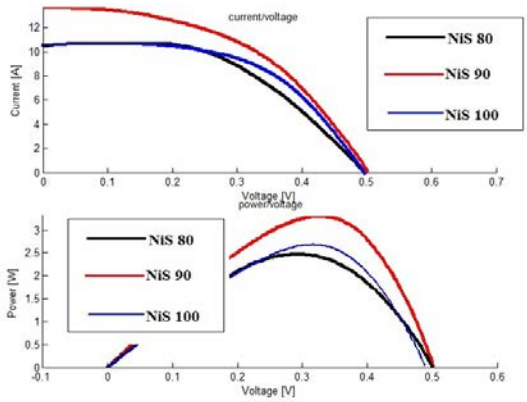

Fig. 5(a) and 5(b) Simulated I–V and PV curves of a QDSSC with different NiS counter electrode deposition temperature

The NiS 90 CE shows the highest catalytic activity, and the NiS 80 and NiS 100 CEs show moderate catalytic activity. The performance increase was caused by the increase in J_{SC}, V_{OC}, and FF with the increase in the temperature. Later, as the temperature was increased further the J_{SC}, V_{OC}, and FF started to decrease. The poorer performance of the Pt CE is due to the strong adsorption of sulfur compounds on the surface of the Pt, which reduces the surface activity and the conductivity of the Pt CE [19].

Parameters	NiS 80	NiS 90	NiS 100	Pt
V_{oc} (V)	0.500	0.502	0.488	0.624
J_{sc} (mAcm-2)	11.30	13.70	11.04	9.12
FF	0.436	0.480	0.496	0.330
η (%)	2.47	3.30	2.67	1.89
R_s (Ω)	7.05	7.03	7.33	9.45
R_{CE} (Ω)	1.02	0.76	0.9	17.34
C_μ (μF)	20.16	56.3	23.71	4.6
Z_w (Ω)	1.47	0.77	0.84	5.22

As a result, a low FF (0.33) is achieved by the Pt CE-based QDSSCs. The photovoltaic results indicate that the NiS 90 acts as an efficient CE for the QDSSC. When the maximum power is similar, the overall efficiency is also similar because it is calculated by the equation as follows:

$$\eta = \frac{P_{MAX}}{P_{IN}} \times 100 \qquad (8)$$

where P_{MAX} is maximum power and P_{IN} is irradiated power into the cell. The power output of QDSSC increases with increase in value of voltage or current. When it reaches a maximum value at optimum value of voltage or current and then starts decreasing, reaches zero value at open circuit voltage or short circuit current so when the temperature was set to 90 °C. The power output reached its peak and the

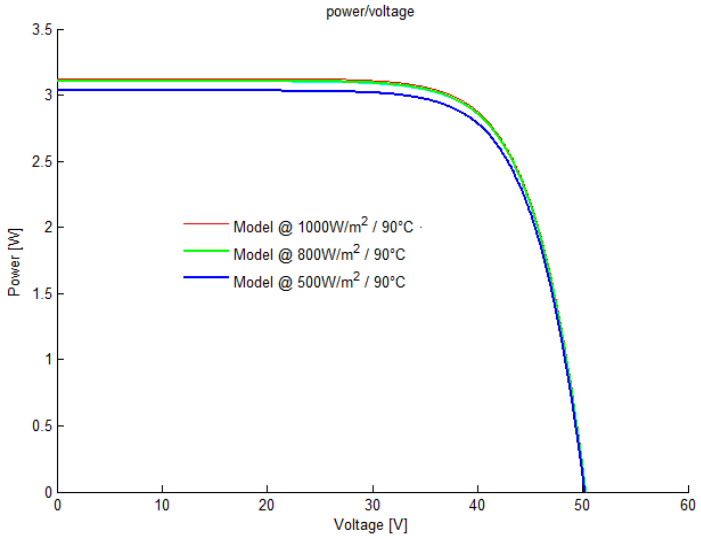

ISSN 2348 – 7968

Fig. 6. characteristics of solar module for varying solar irradiation

temperature was still increased the power output reached its maximum peak and started to decrease as the deposition temperature was increased. Fig. 6, shows that increase in the irradiance leads to a small increase in the open circuit voltage and a large increase in short circuit current. Moreover, the power characteristics also show the aspects including a proportional increase followed by an exponential decrease after attainment of threshold voltage. Increasing solar irradiation impacts positively on the power characteristics, produces high power for a constant voltage.

Electrochemical impedance spectroscopy (EIS) was employed to characterize the charge transfer kinetics of QDSSCs [27]. The obtained Nyquist plots for the frequency range of 100 mHz–500 kHz and in which the inset illustrates the equivalent circuit used to fit the Nyquist plots are shown in Fig. 7a and 7b. Impedance analysis software Z-view was used to model the impedance spectra based on equivalent circuit consisting of a series of two RC circuits with Warburg's impedance (Z_w) as shown in the inset of Fig. 7a. A series resistance (R_s) is added to the circuit to account for the nonzero intercept on the real axis of the impedance plot which represents the sheet resistance of FTO. The electron transfer resistance (R_{CE}) at counter electrode/electrolyte, charge transfer resistance (R_{ct}) at photo electrode/electrolyte interface and the chemical capacitance (C_μ) and Z_w were directly obtained from the fit. Electrochemical parameters determined from EIS analysis are summarized in Table 1. The R_s values of NiS 80, NiS 90 and NiS 100 electrodes are 7.05, 7.03 and 7.33 Ω respectively. The low R_s value could be attributed due to the catalytic material attached to the FTO substrate. The results show that the QDSSCs fabricated using NiS 90 exhibited low value of R_{CE} and Z_w indicating faster electron transport at the interface of CE/electrolyte. The RCE value of the Pt, NiS 80, NiS 90 CE and NiS 100 CEs were found to be 17.34, 1.02, 0.76 Ω and 0.9 Ω, respectively. The lower value of NiS 90 CE confirms that the superior electro catalytic activity in the reduction of polysulfide electrolyte than the Pt, NiS 80 and NiS 100 CEs. The low R_{CE} value indicates an increase in QDSSC efficiency due to the high electron transfer rate at the interface of CE/electrolyte [8]. The higher Z_w value of Pt based QDSSC confirms the inability of electrode with polysulfide electrolyte and leads to a drastic decrease of FF and affecting overall performance of cell [28, 29]. Moreover, high Cμ of NiS 90 QDSSCs is due to higher surface area leading to better catalytic activity [30]. The Cμ values of NiS 80, NiS 90, NiS 100 and Pt CEs were found to be 20.16, 56.3, 23.71 and 4.6 μF respectively. The NiS 90 CE exhibits high Cμ value than the other CEs. The low Z_w value of NiS 90 CE (0.77 Ω) denotes better electrolyte diffusion, facilitates faster mass transport of electron and increases the performance of QDSSC by increasing J_{sc}. Also, the Pt electrode based QDSSC showed large electron transfer resistance at the CE/FTO interface which results in a low FF. The improved J_{sc} and fill factor are due to small electron transfer resistance of the counter electrode and were confirmed through the EIS analysis

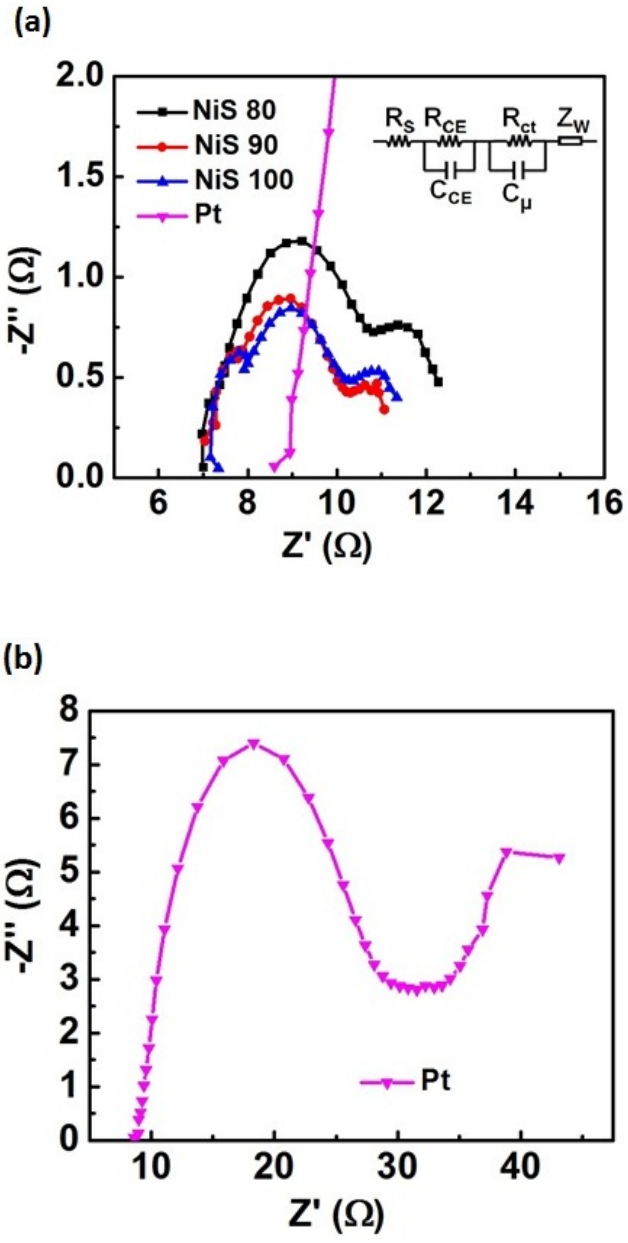

Fig. 7 shows the (a) Nyquist plots of TiO2/CdS/CdSe/ZnS QDSSCs consisting of NiS and (b) Pt electrodes inset shows equivalent circuit.

ISSN 2348 – 7968

.

Fig. 8, shows the Bode plot of NiS CE-based QDSSC. Bode plot is attributed to find the life time of electrons (τe) and this can be calculated using the equation, $\tau_e = 1/2\pi f_{max}$ where f_{max} is the maximum frequency.

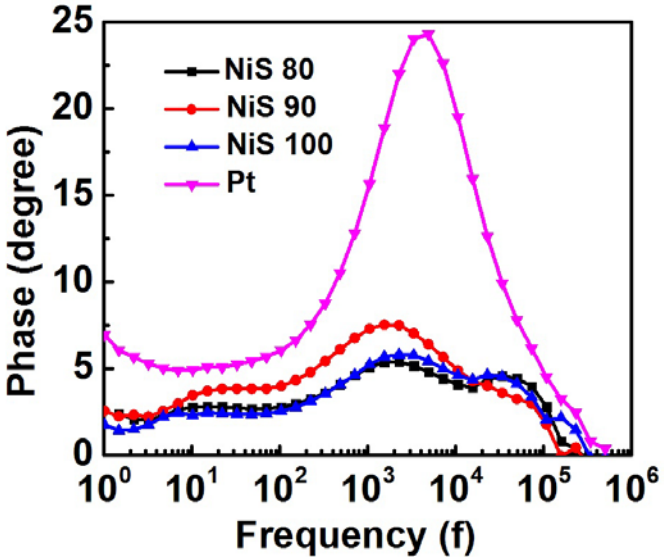

Fig. 8. Bode (frequency) versus phase plots of the QDSSC, obtained from the EIS on NiS CE

The larger the τ_e value in QDSSC the more the electron life time and diffusion rate. The highest electron life time can be seen for NiS 90 (103.37μs) which shows a lower recombination rate with polysulfide Sn^{-2} electrolyte and a faster diffusion rate of electrons [32]. The decreased τ_e is due to increase in the charge recombination rate of the injected electrons at the electrolyte. As shown in the Fig. 6 the τ_e value for NiS 80 (70 μs) and NiS 100 is lower when compared to NiS 90(70 μs)

The absorbance spectra of NiS thin films fabricated at different deposition temperatures are shown in Fig. 9, as shown in this figure, absorbance increases with increase in temperature. These spectra reveal that films, grown under the same parametric conditions have low absorbance in the visible and near infrared regions. However, absorbance in the ultraviolet region is high. Enhanced absorption is observed in the neighborhood of 360 nm. The maximum absorption peak shifts towards the longer wavelength with increase in the deposition temperature. At 550 nm both NiS 90 and NiS 100 seems to be same but as the wavelength increases there was a decrease in the absorbance of NiS 100. Hence we can say NiS 90 has more absorbance when compared to others.

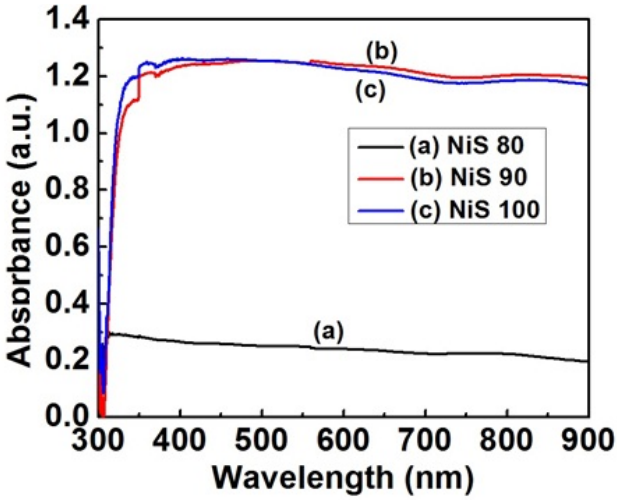

Fig. 9. Shows the absorbance spectra of a NiS counter electrode

5. Conclusion

In this study, the NiS counter electrode deposition temperature was adjusted to improve the efficiency. To simulate the temperature and its improvement, a solar cell with different temperatures (NiS 80, NiS 90, NiS 100) was modeled using the matlab simulink tool. The simulation method was matlab simulink script file on the basis of parameter extraction from experimental data. The simulation showed the I–V and PV characteristics of the cell according to the NiS Counter Electrode temperature with good accuracy. Further, it was confirmed that it is possible to get the highest efficiency at NiS 90 °C from the experimental result of a fabricated module. Results showed that the NiS CE may be suitable to replace the other metal sulfide electrodes and the expensive conventional Pt CE.

Acknowledgement

The authors gratefully acknowledge the contributions of solar cell teammates Pusan National University for their work on the original version of this document

References

[1] R.S. Selinsky, Q. Ding, M.S. Faber, J.C. Wright, S. Jin, Quantum dot nano scale hetero structures for solar energy conversion, Chemical Society Reviews vol. 42, pp. 2963-2985, September 2012.

[2] P.V. Kamat, Boosting the efficiency of quantum dot sensitized solar cells through modulation of interfacial

ISSN 2348 – 7968

charge transfer, Accounts of chemical research, vol. 45 pp. 1906-1915, April 2012.

[3] J.H. Bang, P.V. Kamat, Quantum dot sensitized solar cells. A tale of two semiconductor nanocrystals: CdSe and CdTe, ACS Nano 3 (6), pp. 1467-1476,June 2009.

[4] X. Yu, B. Lei, D. Kuang, C. Su, High performance and reduced charge recombination of CdSe/CdS quantum dot-sensitized solar cells, Journal of Materials Chemistry, vol. 22, pp. 12058-12063, April 2012.

[5] K.G.U. Wijayantha, L.M. Peter, L.C. Otley, Fabrication of CdS quantum dot sensitized solar cells via a pressing route, Solar Energy Materials and Solar Cells, vol. 83, pp. 363-369, December 2003.

[6] N. Fuke, L.B. Hoch, A.Y. Koposov, V.W. Manner, D.J. Werder, A. Fukui, N. Koide, H. Katayama, M. Sykora, CdSe quantum-dot-sensitized solar cell with ˜100% internal quantum efficiency, ACS Nano 4 (11), pp. 6377-6386, October 2010.

[7] K.S. Leschkies, R. Divakar, J. Basu, E.E. Pommer, J.E. Boercker, C.B. Carter, U.R. Kortshagen, D.J. Norris, E.S. Aydil, Photosensitization of ZnO nanowires with CdSe quantum dots for photovoltaic devices, Nano Letters 7(6),
pp. 1793-1798,May 2007.

[8] N. Balis, V. Dracopoulos, K. Bourikas, P. Lianos, Quantum dot sensitized solar cells based on an optimized combination of ZnS, CdS and CdSe with CoS and CuS counter electrodes
Electrochimica Acta, vol. 91, pp. 246-252,February 2013.

[9] M. Nikumbh, V. Gore, R. B. Gore, Structural, optical and photo electrochemical studies of the cadmium sulphide films grown by chemical bath deposition, Renewable Energy, vol. 11, pp. 459-467, August 1997.

[10] Q. Shen, J. Kobayashi, L.J. Diguna, T. Toyoda, Effect of ZnS coating on the photovoltaic properties of CdSe quantum dot-sensitized solar cells, Journal of Applied Physics, vol. 103, 084304.

[11] P.K. Santra, P.V. Kamat, Mn-Doped Quantum Dot Sensitized Solar cells: A strategy to Boost Efficiency over 5%, Journal of the American Chemical Society, vol. 134, pp. 2508-2511, January 2012.

[12] Y.-L. Lee, Y.-S. Lo, Highly efficient quantum-dot-sensitized solar cell based on co-sensitization of CdS/CdSe, Advanced Functional Materials, vol. 19, pp. 604-609, February2009.

[13] N. Guijarro, J.M. Campina, Q. Shen, T. Toyoda, T. Lana-Villarreal, R. Gomez, Uncovering the role of the ZnS treatment in the performance of quantum dot sensitized solar cells, Physical Chemistry Chemical Physics, vol. 13,
pp. 12024-12032, May 2011

[14] , C. Pejoux, S. Rühle, D. Cahen, G. Hodes, Chemical bath deposited CdS/CdSe-sensitized porous TiO2 solar cells, Journal of Photochemistry and Photobiology A: Chemistry, vol. 181, pp. 306-313, July 2006

[15] S. Giménez, I. Mora-Seró, L. Macor, N. Guijarro, T. Lana-Villarreal, R. Gómez, L.J. Diguna, Q. Shen, T. Toyoda, J. Bisquert, Improving the performance of colloidal quantum-dot-sensitized solar cells, Nanotechnology , vol. 20, 295204, 2009 .

[16] S.S. Kalanur, S.Y. Chae, O.S. Joo, Transparent Cu1.8S and CuS thin films on FTO as efficient counter electrode for quantum dot solar cells, Electrochimica Acta ,vol. 103, pp. 91-95, 2013.

[17] H. K. Mulmudi, S. K. Batabyal, M. Rao, R. R. Prabhakar, N. Mathews, Y. M. Lam, S. G. Mhaisalkar, Solution processed transition metal sulfides: application as counter electrodes in dye sensitized solar cells (DSCs), Phys. Chem. Chem. Phys,vol.13, pp.19307-19309, September 2011.

[18] H. Chen, L. Zhu, H. Liu, W. Li, Efficient iron sulfide counter electrode for quantum dots-sensitized solar cells, Journal of Power Sources, vol. 245, pp. 406-410, January 2014.

[19] Z. Yang, C.Y. Chen, C.W. Liu, H.T. Chang, Electrocatalytic sulfur electrodes for CdS/CdSe quantum dot-sensitized solar cells, Chemical Communications, vol. 46, pp. 5485-5487, June 2010.

[20] V.G. Pedro, X. Xu, I.M. Sero, J. Bisquert, Modeling High-Efficiency Quantum Dot Sensitized Solar Cells, ACS nano 4 (Article), pp.5783-5790, September 2010.

[21] Z. Tachan, M. Shalom, I. Hod, S. Rühle, S. Tirosh, A. Zaban, PbS as a highly catalytic counter electrode for polysulfide-based quantum dot solar cells, Journal of Physical Chemistry C , vol. 115, pp. 6162-6166, March 2011.

[22] L. Han, N. Koide, Y. Chiba, A. Islam, T. Mitate, Modeling of an equivalent circuit for dye-sensitized solar cells: improvement of efficiency of dye-sensitized solar cells by reducing internal resistance, Comptes Rendus Chimie, vol. 9,
pp. 645-651, May-June 2006.

[23] N. Koide, A. Islam, Y. Chiba, L. Han, Improvement of efficiency of dye-sensitized solar cells based on analysis of equivalent circuit, Journal of photochemistry and photobiology A:Chemistry , vol.182, pp. 296-305, September 2006.

[24] H. Seo, M.K. Son, J.K. Kim, J. Choi, S. Choi, S.K. Kim, H.J. Kim, Analysis of cur-rent loss from a series–parallel combination of dye-sensitized solar cells using electrochemical impedance spectroscopy, Photonics and Nanostructures, vol. 10 , pp. 568-574, October 2012.

[25] K.J. Lee, J.H. Kim, H.S. Kim, D. Shin, D.W. Yoo, H.J. Kim, A study on a solar simulation for dye sensitized solar cells, International Journal of Photo energy, vol. 2012 , 834347,December 2011.

[26] CIGRE TF38.01.10 “Modeling New Forms of Generation and Storage”, November 2000

[27] I.M. Sero, S. Gimenez, F.F. Santiago, R. Gomez, Q. Shen, T. Toyoda, J. Bisquert, Recombination in Quantum Dot Sensitized Solar Cells, Accounts of chemical research, vol. 42 pp. 1848-1857, September 2009.

[28] J. Kim, H. Choi, C. Nahm, C. Kim, S. Nam, S. Kang, D.R. Jung, J.I. Kim, J. Kang, B.Park, The role of a TiCl4 treatment on the performance of CdS quantum-dot-

ISSN 2348 – 7968

sensitized solar cells Journal of Power Sources vol. 220 , pp. 108-113, December 2012..

[29] J. Dong, S. Jia, B. Li, J. Zheng, J. Zhao, Z. Wang, Z. Zhu, Journal of Materials Chemistry Nitrogen-doped hollow carbon nanoparticles as efficient counter electrodes in quantum dot sensitized solar cells vol. 22, pp. 9745-9750, March 2012

[30] S. Srinivasa Rao, Chandu. V.V.M. Gopi, Soo-Kyoung Kim, Min-Kyu Son, Myeong-Soo Jeong, A. Dennyson Savariraj, K. Prabakar, Hee-Je Kim, Electrochimica Acta vol. 133, pp. 174–179 , April2014.

Dinah Punnoose received Bachelor's degree in computer science and engineering from Anna University, India and master's degree from Sastra University, India. She is currently pursuing doctor's degree from Electrical and computer engineering in Pusan Nation University, Busan, South korea. Her research interests include modeling and experimental analysis of DSSCs, QDSSCs and pervoskite solar cells

Hee Je kim complted his BS and MS degree from electrical engineering Pusan national university, Busan Korea and doctors degree in electrical engineering from Kyushu university, Japan. He is currently working as a professor in Pusan National University.

Sang-Hwa Chung completed his BS in Electrical Engineering, Seoul National University, asters in Computer Science from Iowa State University He completed his Masters and doctors degree in Computer Science and Engineering from University of Southern California He is currently working as a professor in Pusan National University.